Morphological and Molecular Analysis of Osteoblasts Differentiated from Mesenchymal Stem Cells in Polycaprolactone/Magnesium Oxide/Graphene Oxide Scaffold

Z. Niknam[1,2],
H. Zali[2,3]*,
V. Mansouri[1,2],
M. Rezaei Tavirani[2],
M. Omidi[4]

[1]*Faculty of Paramedical Sciences, Shahid Beheshti University of Medical Sciences, Tehran, Iran*
[2]*Proteomics Research Center, Shahid Beheshti University of Medical Sciences, Tehran, Iran*
[3]*Department of Tissue Engineering and Applied Cell Sciences, School of Advanced Technologies in Medicine, Shahid Beheshti University of Medical Sciences, Tehran, Iran*
[4]*Protein Research Center, Shahid Beheshti University, GC, Tehran, Iran*

ABSTRACT

Background: The loss or dysfunction of bone tissue that observed after bone tumor resections and severe nonunion fractures afflicts 200 million people worldwide. Bone tissue engineering is a promising approach to repair osteoporotic fractures.

Objective: In this paper, polycaprolactone (PCL)/magnesium oxide (MgO)/graphene oxide (GO) nanofibrous scaffold was fabricated by electrospining method, and its biocompatibility and osteogenic differentiation of adipose-derived mesenchymal stem cells (MSCs) on this scaffold were evaluated and compared with pure PCL nanofibrous scaffold.

Methods: SEM analysis, DAPI staining and MTT assay were used to evaluation biocompatibility of PCL/MgO/GO composite scaffold. In addition by ALP assay and proteomic approach, osteostimulatory effect of electrospun composite scaffold was investigated and the expression level of osteogenic markers including Runt-related transcription factor cbfa1/runx2 (runx2), collagen type I (Col1a1) and osteopontin (OPN) in MSCs seeded on PCL/MgO/GO composite scaffold was determined and compared with pure PCL scaffold. Then, RT-PCR technique was used to validate the level expression of these genes.

Results: The obtained results showed that adhesion, viability and ALP activity of MSCs on PCL/MgO/GO scaffold considerably enhanced compared with pure PCL. As well as proteomic and real-time analysis illustrated the expression of osteogenic markers including runx2, Col1a1 and OPN increased (>2-fold) in cells seeded on PCL/MgO/GO composite scaffold.

Conclusion: It was concluded that MgO and GO nanoparticles could improve the biocompatibility of PCL scaffold and enhance the osteogenic differentiation of MSCs.

KEYWORDS: Bone tissue engineering; Scaffold; Proteomics; Mesenchymal stem cells; Osteoblast

INTRODUCTION

In the last decades, bone tissue engineering (BTE) has been increasingly used for the bone reconstitution and treatment of bone defects. This new strategy has been used as a substitution for the traditional bone repair procedures including autografts (from the patient iliac crest) and allografts (from the cadaver bone) [1]. Several problems have been reported with autografts and allografts. Those include variable resorption, risk of donor site morbidity, high rate of failure in specific sites and the need for a second surgery, minor immunogenic rejection and the risk of disease transmission [2]. BTE methods do not have these limitations and open a new avenue for the regeneration and repair of bone injuries. This provides a hybrid con-

*Correspondence: Hakimeh Zali, Proteomics research center, Shahid Beheshti University of Medical sciences, Tehran, Iran
E-mail: hakimehzali@gmail.com

struct including cells and gene-activating materials to induce regeneration and slowly replacing the missing bone with the newly formed tissue [3]. A scaffold in BTE can be defined as a specific environment and architecture to support the three-dimensional (3D) tissue formation and development [4, 5]. A suitable scaffold for BTE applications should have characteristics such as being biocompatible, bioresorbable, biodegradable, non-toxic, non-immunogenic, and improve cell viability, attachment, proliferation, and differentiation [2]. MSCs represent a great potential for regeneration of bone since the 1980s [6]. At present, various scaffolds applicable to BTE are polymers, bioactive ceramics (glasses) and hybrids (composites) [7, 8]. In this research magnesium oxide (MgO) and graphene oxide (GO) nanoparticles were used to incorporate into a polycaprolactone (PCL) polymer, to fabricate a biocompatible composite scaffold that significantly induced differentiation of MSCs to osteoblast. The PCL polymer has widely been used to fabricate various scaffolds, due to its appropriate properties for tissue engineering of bone and cartilage [9]. PCL is an FDA-approved bioresorbable and biocompatible polymer with low melting point, which makes its process and blending with other polymers easy [10]. In addition, electrospun PCL nanofibers can mimic the identity of ECM in living tissues and possess an extremely high surface-to-volume ratio [11]. MgO nanoparticles are biodegradable metallic materials essential to the bone development and extracellular matrix formation [12, 13]. GO is a single-layer of aromatic carbon atoms in a two-dimensional lattice, with many unique properties such as ultra-large surface area, rich oxygen-containing functional groups and excellent flexibility [14, 15]. Substrates coated with GO have been demonstrated to improve stem cells differentiation towards multiple specific lineages [16], such as osteogenic, adipogenic, cardiomyogenic, and epithelial genic [17, 18], suggesting GO as a promising base material for building scaffolds and composites for stem cell-based tissue engineering. The present study was conducted to determine the biocompatibility of PCL/MgO/GO nanofibrous scaffold and effect of 0.5% MgO and 0.5% GO nanoparticles in PCL scaffold on the osteogenic differentiation of MSCs compared with pure PCL scaffold. To do so, proteomics approach and RT-PCR validation were used to investigate the targeted genes involved in osteoblasts.

MATERIALS AND METHODS

Fabrication of Electrospun PCL and PCL/MgO/GO Nanofibers

The PCL/MgO/GO nanofibrous scaffolds were prepared using electrospinning method. PCL (number-average molecular weight [Mn] 80,000) was purchased from Sigma-Aldrich. Dimethylformamide (DMF), and chloroform ($CHCl_3$) were purchased from Aladdin (China). The PCL granules were dissolved in DMF:$CHCl_3$ (2:8) to obtain a 10% w/v solution and homogeneous mixture. Afterward, MgO and GO powders were gradually added with the ratio of 1:0.005 w/w. The solution was blended for 30 min using a vortex; then, for obtaining a wholly suspended solution, ultrasonication was applied for 2 hrs. The polymeric mixture was filled into a 10-mL plastic syringe with a 20G stainless steel needle, and then electrospinning was carried out. The syringe tip was charged to a supplied high-voltage (18 kV), and the steady-state flow rate was set to 1 mL/h. The polymer solution was deposited as solid fibers onto a fixed grounded aluminum target at 10 cm from the needle tip. The collected electrospun nanofibers were subsequently vacuum-dried for at least 48 hrs to remove any residual solvents.

Surface Morphologies of the Nanofibers

The surface morphology and diameter of the nanofibers were studied by scanning electron microscopy (SEM, QUANTA-200, FEI, Hillsboro, OR, USA) at an accelerating voltage of 15 kV. Before being observed with SEM, each sample was coated with a layer of gold using a sputter coater.

Isolation of MSCs from Adipose Tissue and Characterization

The animal study was approved by the Ethics Committee of Shahid Beheshti University of Medical Sciences (IR.SBMU.REC.1397.047).

Male Wistar Han rats were housed under the standard condition. The inguinal fat pad from 6-week-old animals was collected under sterile conditions and rinsed with phosphate-buffered saline (PBS) containing 1% antibiotic-antimycotic solution (Sigma) several times to remove all blood vessels and connective tissues. For isolation of MSCs, inguinal adipose tissue was minced into ~1 mm^3 pieces and digested in 0.1% collagenase type 1 (Thermo Fisher Scientific Inc., Waltham, MA) for 30 min at 37 °C with gentle vortex. For neutralization of collagenase activity, an equal volume of DMEM supplemented with 10% fetal bovine serum was added and centrifuged at 1000×g for 5 min at 4 °C. For removal of the solid aggregates, the obtained cell suspension was filtered through a 100-μm cell strainer (BD Falcon, USA) and centrifuged at 2000 rpm for 5 min. The resulting cell pellet was re-suspended in DMEM containing 10% fetal bovine serum, 100 U/mL penicillin, and 0.1 mg/mL streptomycin (all Invitrogen) and incubated at 37 °C with 5% CO_2. The medium was changed every three days, and when the confluency of cells in the flasks was reached to 80%–90%, trypsin-EDTA solution (0.25% trypsin and 1 mM EDTA) was added to passage the flasks. After the 3rd passage, MSCs were washed with PBS and incubated with antibodies against (CD44, CD73, and CD90 [BD Biosciences, Palo Alto, CA, USA]) for 45 min at 4 °C. Flowcytometry detection was performed using a FACs Calibur Cytometer (FC 500; Beckman Coulter, Fullerton, CA, USA).

Study of MSCs Adhesion on Scaffolds

For investigation of cell adhesion on prepared nanofibrous scaffolds, SEM images and DAPI staining were used. MSCs at the density of 10^4 cells/mL were seeded onto each scaffold in a 48-well plate. The MSCs were incubated in medium containing DMEM, 10% fetal bovine serum, 100 U/mL penicillin, and 0.1 mg/mL streptomycin (all Invitrogen) at 37 °C under 5% CO_2 for 1–2 days. For observation of cells with SEM, the cell/scaffold constructs were washed twice with PBS; they were fixed in 2.5% glutaraldehyde solution (Sigma) for 1 hr at room temperature. The excess glutaraldehyde was then removed by washing with PBS and scaffolds were dehydrated in a graded ethanol series. Subsequently, the dried scaffolds were used for SEM viewing.

For recognizing cell attachment in DAPI staining method, the MSCs at a density of 10^4 cells/mL were seeded onto each scaffold in a 48-well plate and cultured in medium containing DMEM, 10% fetal bovine serum, 100 U/mL penicillin, and 0.1 mg/mL streptomycin (all Invitrogen) at 37 °C under 5% CO_2 for 1–2 days. The samples were then washed twice with PBS and fixed with 10% formalin for 30 min. The excess formalin was then removed by washing with PBS, and the cell nuclei were stained with 0.1 μg/mL of DAPI solution for 10 min. Next, the cell-scaffold constructs were rinsed three times with PBS to remove excess DAPI and investigated using a fluorescence microscope (Zeiss Axiovert 200; Carl Zeiss Inc., Thorn -wood, NY, USA).

MTT Assay for Cell Viability

MSCs derived from mouse adipose tissue were seeded onto the PCL and PCL/MgO/GO scaffolds. The culture medium was Dulbecco's Modified Eagle Medium (DMEM) containing 10% fetal bovine serum, 1% antibiotic-antimycotic, and the cells were incubated at 37 °C with 5% CO_2. For the evaluation of cell viability on nanofibrous scaffolds, MTT (3-[4, 5-dimethylthiazol-2-yl]-2, 5-diphenyltetrazolium bromide) assay was applied. MSCs were cultured in 96-well plates at an initial seeding density of 10^4 cells/cm^2 for 1, 4 and 7 days. In this assay, the culture medium in the disks was aspirate and cells/scaffold constructs rinsed by PBS, and 100 μL RPMI1640 (Bio-IDEL) was added to each well. Then, 10 μL of MTT solution (5 mg/mL) was added to the culture wells and incubated for 4 hrs at 37 °C and 5% CO_2. The formation of water-insoluble formazan purple-colored crystals implies the presence of viable cells. The crystals were dissolved by adding 100 μL dimethyl-sulfoxide (DMSO, Merck, Germany) to each well, incubating at 37 °C and 5% CO_2 for 10 min. Finally, the absorbance value was recorded by an ELIZA reader (URIT-660, China) at a visible absorption wavelength of 570 nm and with 630 nm

Table 1: Primer sequences

Runx2	F	5'-TCCCCATCCATCCATTCCAC-3'
	R	5'-GGTGGCAGTGTCATCATCTG-3'
Col1a1	F	5'-GCCAAGAAGACATCCCTGAAG-3'
	R	5'-TAGCACGCCATCGCACAC-3'
OPN	F	5'-GAGGGCTTGGTTGTCAGC-3'
	R	5'-CAATTCTCATGGTAGTGAGTTTTCC-3'
Hprt1	F	5'-CCAGCGTCGTGATTAGTG-3'
	R	5'-CGAGCAAGTCTTTCAGTCC-3'

filter as a reference wavelength. The cell viability was determined by the optical densities.

Alkaline Phosphatase Activity (ALP)

Alkaline phosphatase activity was determined to evaluate the osteogenic differentiation of MSCs seeded on PCL and PCL/MgO/GO scaffolds. For this purpose, MSCs (10^5 cells/mL) were seeded on scaffolds in 24-well plates and incubated in complete growth media (containing DMEM, 10% fetal bovine serum and 100 U/mL penicillin, 0.1 mg/mL streptomycin, and osteogenic differentiation supplements including 50 mM ascorbic acid, 10 mM β-glycerophosphate, and 0.1 mM dexamethasone) at 37 °C under 5% CO_2. After 7 and 14 days of culture, cells were lysed with 1× RIPA buffer. Lysates were mixed with p-nitrophenyl phosphate solution for 30 min at 37 °C. Reactions were stopped with 500 µL 1-N NaOH. The absorbance of reaction solutions was measured using a plate reader at 405 nm. For measurement of total protein content in each sample, Bradford protein assay reagent (Thermo Fisher Scientific) was used. The amount of ALP activity was normalized to the total amount of protein concentration per well and expressed as U/mg protein.

Protein Extraction and Separation by Two-dimensional Gel Electrophoresis

For protein extraction, MSCs (10^5 cells/mL) were seeded onto the PCL and PCL/MgO/GO scaffolds in 24-well plates. The cells were incubated in complete growth media (containing DMEM, 10% fetal bovine serum, 100 U/mL penicillin, 0.1 mg/mL streptomycin, and osteogenic differentiation supplements including 50 mM ascorbic acid, 10 mM β-glycerophosphate, and 0.1 mM dexamethasone) at 37 °C under 5% CO_2. After 14 days the cells were lysed and harvested in a buffer containing 7 M urea, 2 M thiourea, 4% w/v 3-([3-cholamidopropyl] dimethyl ammonio) propane sulfonate (CHAPS), 0.2% 100× Bio-Lyte 3/10, 65 mM dithiothreitol (DTT), 1% (v/v) protease inhibitor cocktail (Sigma, USA) and ampholyte. The lysates thoroughly were dissolved with repeated vortex and ultra-sonication. After 4 hrs of incubation on ice, due to removing insoluble substances, the lysates were centrifuged at 16,000×g for 30 minutes at 4 °C. The total protein concentration of samples was estimated by the Bradford assay.

For two-dimensional electrophoresis, the isoelectric focusing as the first dimension was performed using 11 cm, PH 3-10 IPG strips. To reach a final protein amount to 1200 µg/strip, samples were diluted in a solution containing rehydration buffer, IPG buffer, and DTT. Next, gels were incubated in equilibration buffer I (6 M urea, 2% SDS, 0.375 M Tris HCl pH 8.8, 20% glycerol, 130 mM DTT) for 15 min, and then for 15 min alkylated in the same buffer with 2.5% iodoacetamide instead of DTT. In the second dimension, 12% SDS-polyacrylamide slab gels were used, and treated strips were transferred on the surface of these gels and sealed with 1% agarose. The gels ran in SDS electrophoresis buffer (25 mM Tris base, 192 mM glycine, 0.1% SDS) in 2.5 W for 30 min and then 15 W. After electrophoresis gels were stained with Coomassie Brilliant Blue. Following the de-staining process, the gels were placed in 10% acetic acid overnight. Gels were scanned using Bio-Rad Image Scanner and to identify spots differentially expressed between cells on PCL and PCL/MgO/GO scaffolds based on their volume and density,

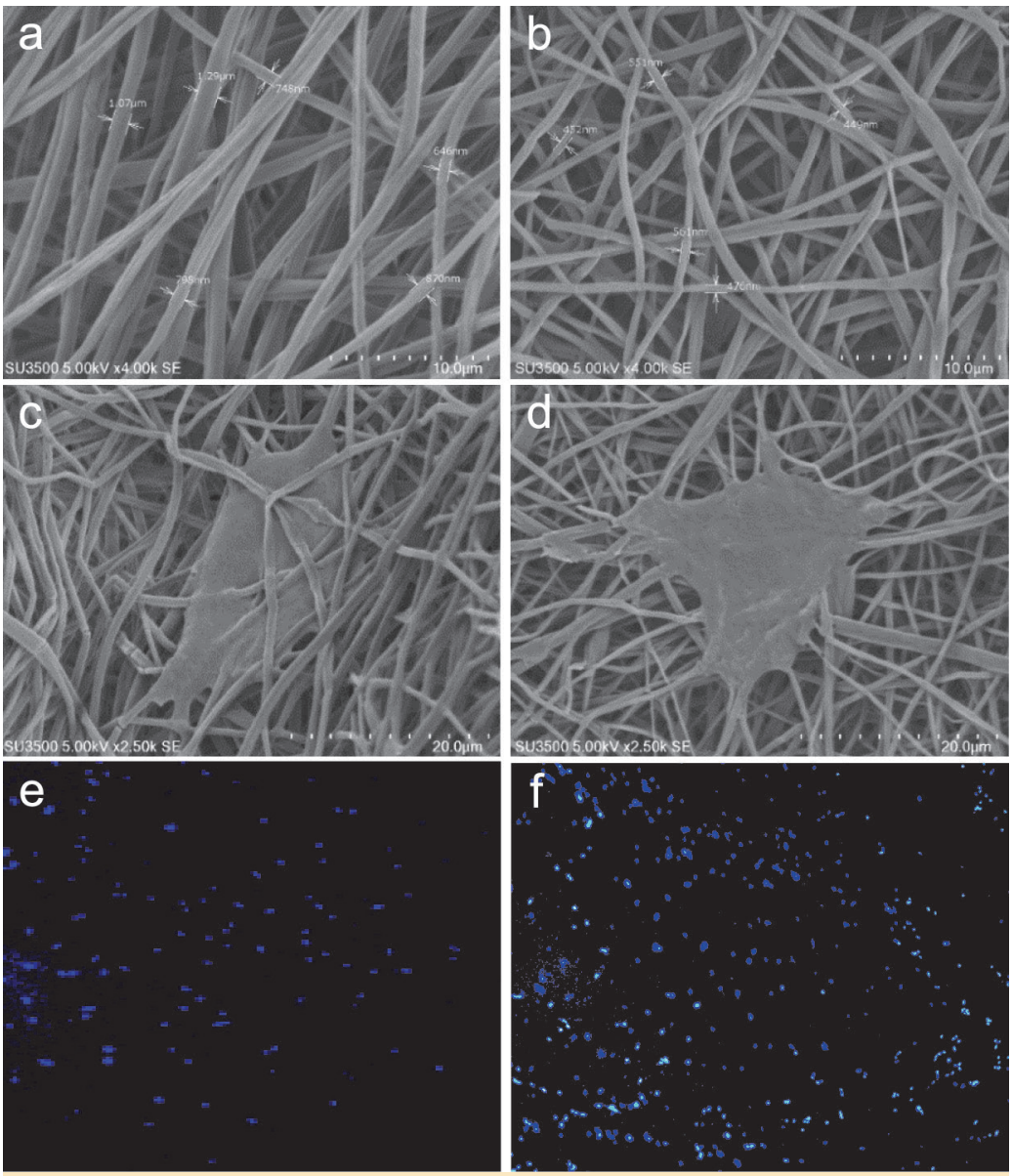

Figure 1: Surface morphological and constructional images of nanofibers by SEM: a) PCL, b) PCL/MgO/GO. Original behaviors of MSCs on nanofibrous scaffolds; SEM images after 1 day of culture: c) PCL, d) PCL/MgO/GO. Fluorescence microscope images for DAPI staining of MSCs cultured for 1 day on nanofibrous scaffolds: e) PCL, f) PCL/MgO/GO.

the images were analyzed by Progenesis Same spot software. The conventional method of computerized analysis to do so is spot finding, image warping, matching, and quantification in conjunction with detailed manual checking.

Real-time Reverse Transcriptase Polymerase Chain Reaction (RT-PCR)

Total RNA was extracted from MSCs (10^5 cells/mL) seeded on PCL and PCL/MgO/GO scaffolds using the RNeasy mini kit (Qiagen) on the 7^{th} and 14^{th} days. The RNA concentration was determined in a NanoDrop spectrophotometer. The RNA was then reverse transcribed with RevertAid™ First Strand cDNA Synthesis kit (ABI) following the manufacturer's instructions. Finally, real-time RT-PCR was applied using the SYBR Green PCR Master Mix (All-in-One™ qPCR Mix, GeneCopoeia, USA) by ABI PRISM 7500 sequence detection system (Applied Biosystems, CA, USA). The expression data of target genes were normalized to hypoxanthine phosphoribosyltransferase 1 (hprt1) as a housekeeping

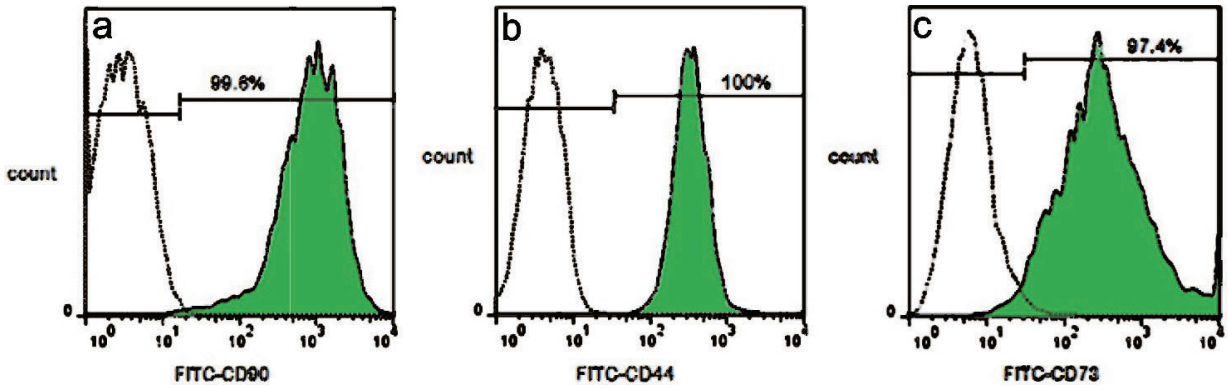

Figure 2: Flowcytometry analysis of MSCs labeled with a) CD90, b) CD44, and c) CD73 conjugated to FITC

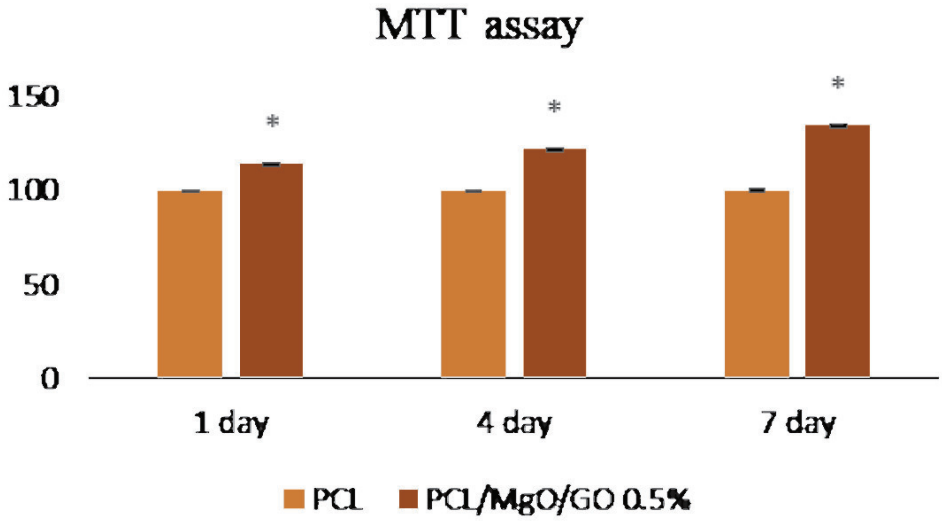

Figure 3: Viability percentage of MSCs on PCL and PCL/MgO/GO scaffolds on the 1st, 4th, and 7th days (*p<0.05)

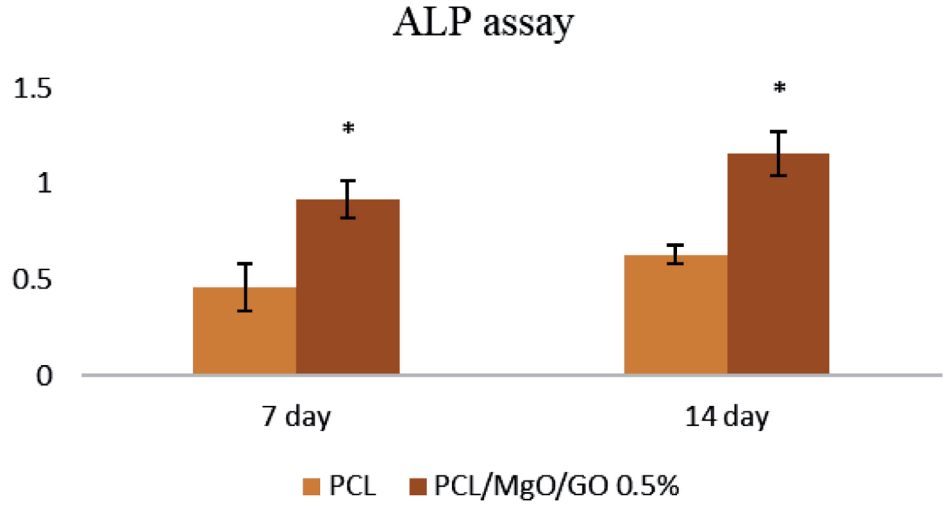

Figure 4: ALP activity of MSCs grown on PCL and PCL/MgO/GO (0.5%) nanofibrous scaffolds on the 7th and 14th days (*p<0.05)

gene, and the $2^{-\Delta\Delta Ct}$ method was used to calculate the relative quantification of target genes. The primers sequences used in this study are shown in Table 1.

Statistical Analysis

All experiments were done in triplicate. The results were expressed as mean±SD. One-way analysis of variance (ANOVA) was used to determine the statistical differences. A p value <0.05 was considered statistically significant.

RESULTS

Morphologies of the Nanofiber

Figure 1 shows the SEM images of the electrospun PCL and PCL/MgO/GO (0.5%) nanofibrous scaffolds. A random fibrous network was achieved by electrospinning of PCL and PCL/MgO/GO solutions. PCL/MgO/GO nanocomposite fibers indicated a 3D interconnected porous structure similar to pure PCL. The average diameter of the collected fibres was quantified. The diameter of nanocomposite fibers significantly decreased in comparison with PCL nanofibres. The overall morphologies of the PCL/MgO/GO nanocomposite scaffolds were better.

Surface Protein Markers

Flowcytometry analysis of MSCs surface marker expression showed that cells were 99.6% positive for CD90, 100% positive for CD44, and 97.4% positive for CD73, which were all adipose-derived MSCs surface protein markers (Fig 2).

Adhesion, and Cell Viability of MSCs

Figure 1 shows the SEM images of cell morphology of MSCs seeded on PCL and PCL/MgO/GO nanofibers after one day of culture. These images indicated that MSCs were successfully adhered to both nanofibrous scaffolds. There was a considerable difference in cell morphology depending on the surface structure and chemistry the cells were in contact with. MSCs that were cultured on PCL/MgO/GO scaffold spread in many directions and appeared much more mature and flattened in comparison with those adhered to pure PCL. Images of DAPI staining showed that only a small population of MSCs were adhered on PCL scaffold, while on the entire surface of PCL/MgO/GO nanofiber materials, more MSCs were attached (Fig 1).

Before investigating the osteogenic differentiation of MSCs on scaffolds and their protein profile, it is crucial to evaluate the cytotoxicity of scaffolds by quantitative analysis using the MTT assay. Figure 3 shows the results of MTT assay at 1, 4, and 7 days. PCL/MgO/GO scaffolds containing 0.5% nanoparticles showed enhanced cell viability in MSCs compared with the pure PCL scaffolds as control; the proliferation of cells on PCL/MgO/GO scaffolds gradually increased.

Osteogenic Differentiation

Figure 4 shows the ALP activity of MSCs subjected to nanofiber scaffolds at 7 and 14 days. When the MSCs were introduced into PCL/MgO/GO scaffolds, the ALP activity of stem cells was notably elevated in comparison with PCL nanofibers. This proves that MgO and GO nanoparticles in PCL scaffolds are able to induce ALP activity as a marker of early osteoblastic differentiation. The expression of ALP in MSCs grown on nanofibrous scaffolds at 14 days was enhanced compared with those at 7 days; this increase in the PCL/MgO/GO scaffolds was more evident.

Proteomic Analysis

The extracted protein from cells on PCL and PCL/MgO/GO scaffolds was separated using a 2-DE technique; the protein expression pattern was compared between two samples using Progenesis Same Spots software. The findings illustrated that gene expression was affected when MSCs were exposed to MgO and GO nanoparticles (Fig 5).

Simple statistical tests were applied to establish a putative hierarchy in which the variation in protein level was ranked conforming to a cut-off point with $p<0.05$. Among the statistically significant protein spots ($p<0.05$), three spots related to runx2 (IP 9.37 and MW 66.2), Col1a1 (IP 5.65 and MW 138.013) and OPN (IP 4.53 and MW 37.25) were definitely de-

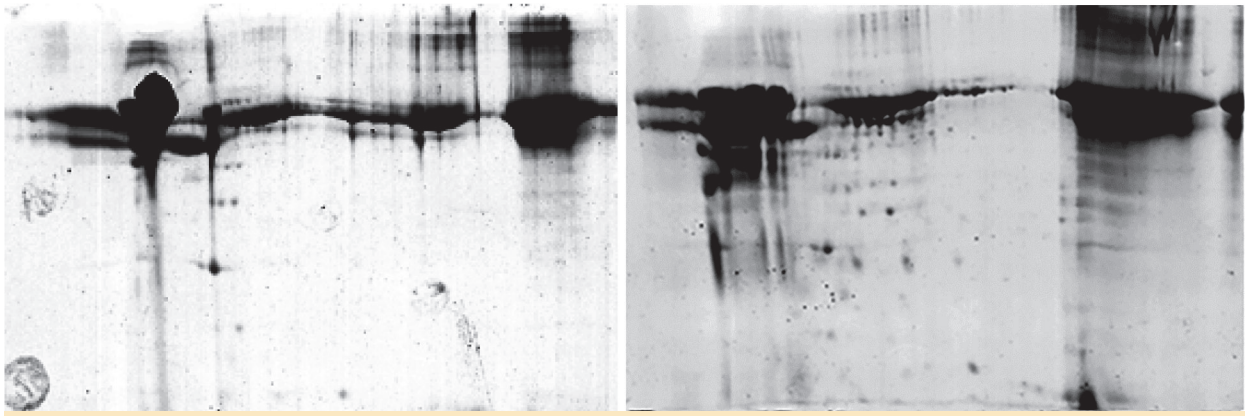

Figure 5: 2DE gel images of a) MSCs on PCL scaffold, and b) MSCs on PCL/MgO/GO scaffold

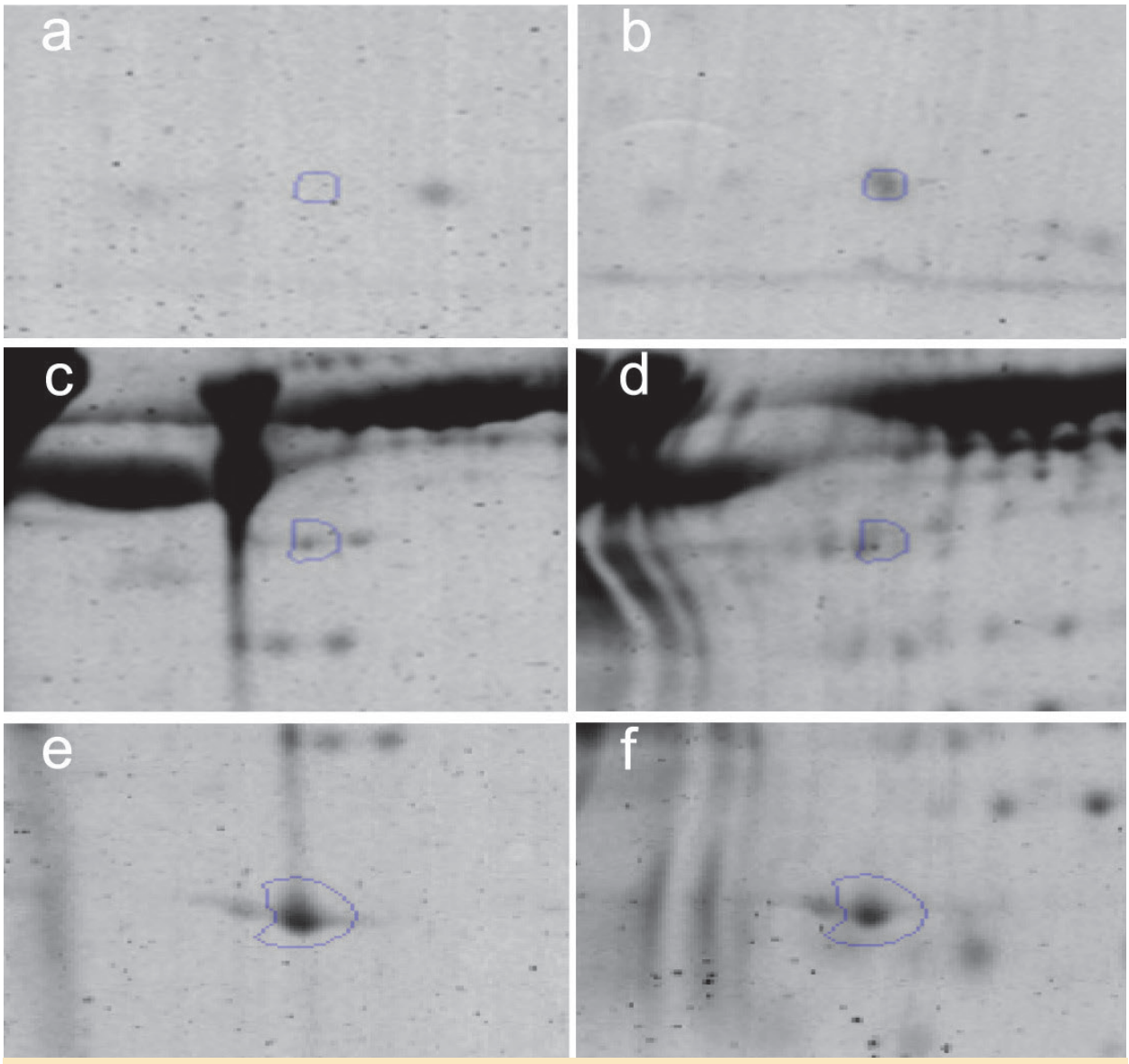

Figure 6: Images of protein spots: runx2 a) PCL; b) PCL/MgO/GO, Col1a1; c) PCL; d) PCL/MgO/GO, OPN; e) PCL; and f) PCL/MgO/GO

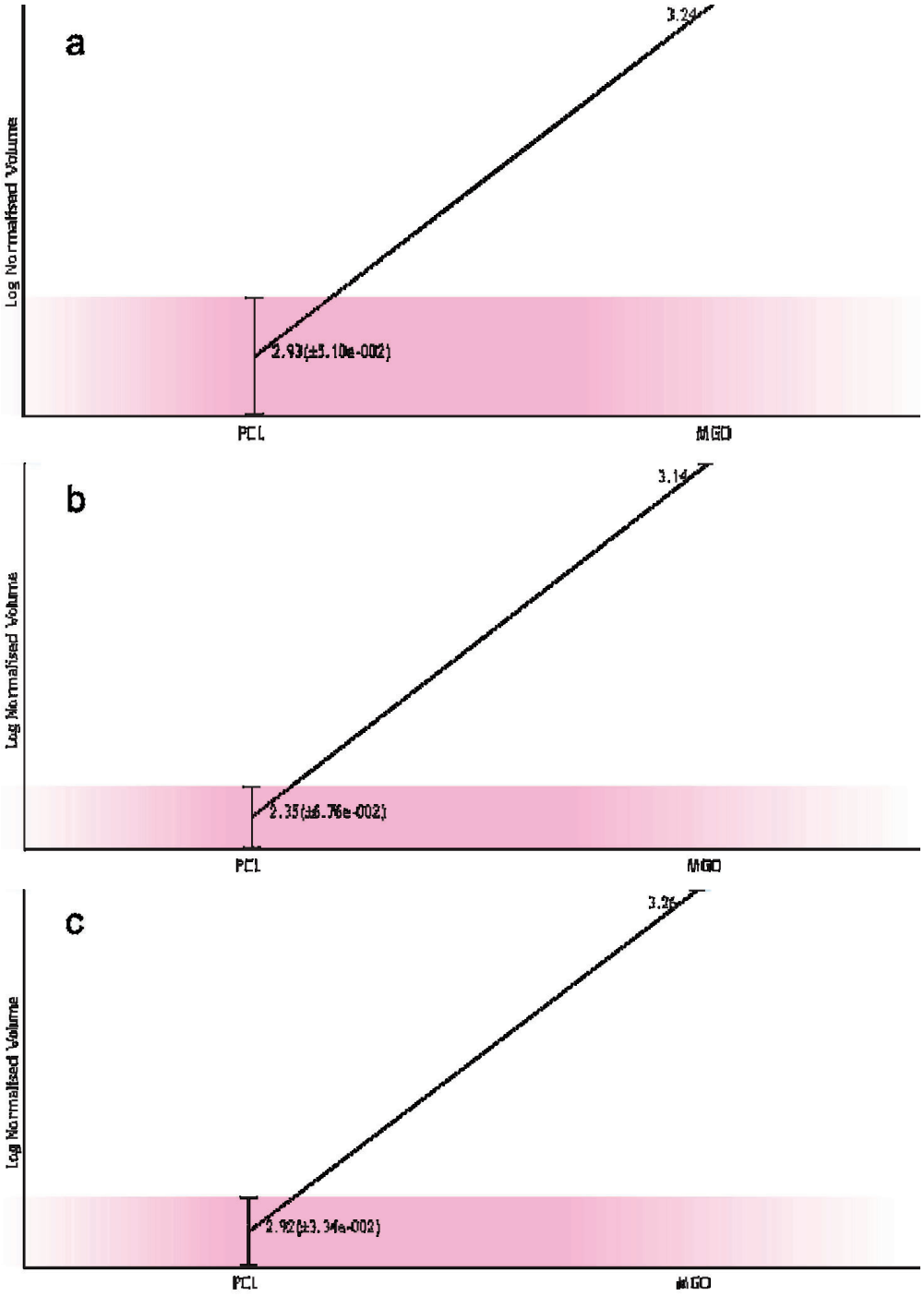

Figure 7: Targeted proteins have more than 2-fold up-regulation: a) runx2, b) Col1a1, c) OPN in PCL/MgO/GO scaffold compared with pure PCL

tected, which have an up-regulation (>2-fold) in PCL/MgO/GO scaffold compared with PCL scaffold (Figs 6 and 7).

RT-PCR Validation

Analysis of steady-state mRNA levels for the classical markers of osteoblast differentiation, including runx2, Col1a1, and OPN were carried out to validate the differentially expressed proteins at the transcription level (Fig 8). The obtained results indicated that the increase observed in the expression of these genes in PCL/MgO/GO scaffold was much higher than that recorded in cells on PCL scaffold at 7 and 14 days.

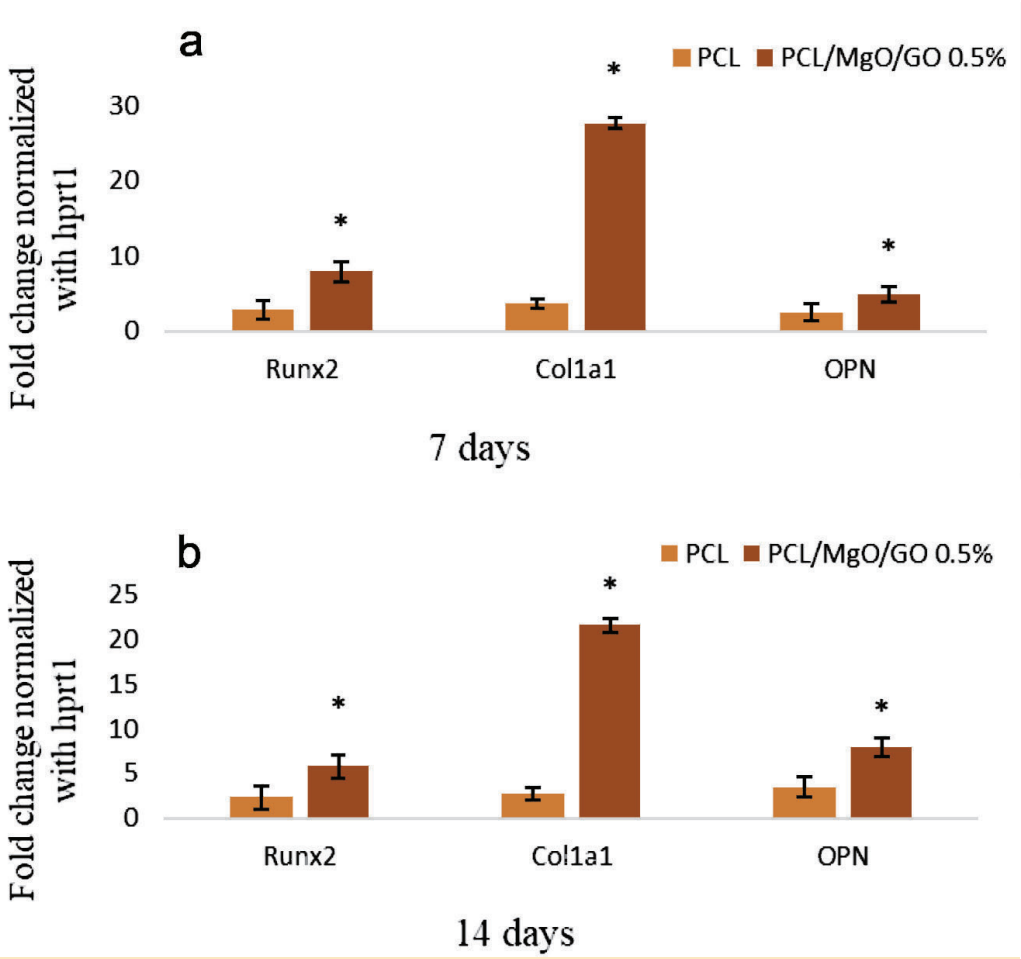

Figure 8: Various mRNA expression changes of MSCs in response to PCL and PCL/MgO/GO scaffolds on a) 7th day and b) 14th day (*p<0.05)

DISCUSSION

Previous studies report that nanoscale materials can induce changes in the cell adhesion [19], morphology [20], proliferation, marked differentiation marker activity [21], cytoskeleton network, and nuclear organization [22]. To investigate possible effects of MgO and GO nanoparticles in PCL scaffold on osteogenic differentiation of MSCs, analysis of biocompatibility of these scaffolds and targeted protein expression involved in osteoblast and RT-PCR validation were carried out. SEM analysis of electrospun nanofibers illustrated uniform small MgO and GO loaded fibers. Suryavanshi, *et al*, report the reduction in fiber diameter of pure PCL with incorporation of MgO nanoparticles [21]. A decrease in average diameter of the PCL/GO composite nanofibers in comparison with the pure PCL has been reported by Song, *et al* [23]. The decrease in the diameter of composite nanofibers could be attributed to electronic conductivity of the composite solution due to the incorporation of MgO and GO nanoparticles. Mg and O ions in the polymer solution increase the density of the charge; GO is a good conductive material. Therefore, these parameters of solution could influence the elongation and thinness of the straight jet portion and the diameter of the nanofibers. Reduction in fiber diameter increases the surface area to volume ratio and fiber interaction points with cells. SEM observation of nanofibrous scaffolds and DAPI staining after seeding of MSCs, as well as MTT assay results, indicated that adhesion, spreading, and proliferation of MSCs on PCL/MgO/GO scaffold were improved compared with that when a pure PCL scaffold was used. The initial phase of cell-scaffold interactions is crucial for subsequent cellular processes such as proliferation and differentia-

tion. GO with oxygen-containing functional groups affects the surface roughness and hydrophilicity of nanofibres and increases the adsorption of serum proteins and induces cell adhesion and proliferation. In addition, MgO nanoparticles increase the rough surface for higher protein adsorption and enhance water adsorption and hydrophilicity that induce cell attachment, proliferation, and differentiation. All these interesting properties considerably enhanced the osteostimulatory effect of PCL scaffold due to the incorporation of GO and MgO nanofillers. GO with oxygen-containing functional groups can have high interactions with proteins by covalent, electrostatic and hydrogen bonds [24]. On the other hand, through π-π stacking between the aromatic rings in the biomolecules and the basal plane of GO, osteogenic inducers (dexamethasone and β-glycerophosphate) were pre-concentrate and subsequently, osteogenic differentiation was increased. Runx2, Col1a1, and OPN are commonly used as osteogenic differentiation markers [25, 26]; in this study, 2DE gel analysis demonstrated that expression of these proteins was increased by >2-fold in cells on PCL/MgO/GO scaffold compared with the pure PCL scaffold. Runx2 is a transcription factor that was often referred to as the master switch of osteogenic differentiation [27]. This protein contains a highly conserved Runt domain that acts as the DNA binding domain [28]. Runx2 can directly regulate transcription of osteocalcin (OCN), Col1a1, OPN and collagenase 3 genes that are related to osteoblast differentiation, through binding to specific enhancer regions containing a core sequence, PuCCPuCA [29]. Previous studies illustrate that there is no simple correlation between runx2 protein levels and expression of its target genes. Functions of this transcription factor depend on post-translational modification or protein-protein interactions. Runx2 protein must create a heterodimer with transcriptional coactivator core binding factor β(Cbfβ), as a cotranscription factor due to binding to DNA. In osteogenic differentiation process, Runx2 activates and regulates many signaling pathways such as transforming growth factor-β 1 (TGF-β1), BMP, Wingless-type (Wnt), Hedgehog (HH), and (Nel)-like protein type 1 (NELL-1) [30]. Col1a1 proteins were synthesized by osteoblasts that make up 90% of the proteins in the bone matrix and have fibrillar structures. Fibrous extracellular matrix proteins such as Col1a1 mechanically support cells and form the basis of tissue shape by forming complex 3D scaffolds [31]. OPN is one of the abundant non-collagenous extracellular matrix proteins that could play a role in meditation of the mechanical stress signals to osteoblasts. OPN is considered a phenotypic marker of fully differentiated osteoblastic cells. Growth factors particularly TGF-β and physical stress, which promote bone matrix formation, can stimulate OPN synthesis [32]. Due to better cell attachment and increase expression of ALP, runx2, Col1a1, and OPN as markers of osteogenic differentiation on PCL/MgO/GO scaffold compared with pure PCL scaffold, proved by RT-PCR validation, it was concluded that MgO and GO nanoparticles increase biocompatibility of PCL scaffold and induce osteogenesis.

ACKNOWLEDGMENTS

This work was supported by the Proteomics Research Center, Shahid Beheshti University of Medical Sciences.

REFERENCES

1. Stevens MM. Biomaterials for bone tissue engineering. *Materials today* 2008;**11**:18-25.
2. Roseti L, Parisi V, Petretta M, *et al*. Scaffolds for Bone Tissue Engineering: State of the art and new perspectives. *Materials Science and Engineering Mater Sci Eng C Mater Biol Appl* 2017;**78**:1246-62. doi: 10.1016/j.msec.2017.05.017
3. Xu W, Liao X, Li B, Li T. Biomaterials and bone tissue engineering. Bioelectronics and Bioinformatics (ISBB), 2011. International Symposium on bioelectronics and bioinformatics 2011: 224-7.
4. Bouët G, Marchat D, Cruel M, *et al*. In vitro three-dimensional bone tissue models: from cells to controlled and dynamic environment. *Tissue Engineering Part B: Reviews* 2014;**21**:133-56.
5. Navarro M, Michiardi A, Castano O, Planell J. Biomaterials in orthopaedics. *Journal of the Royal Society Interface* 2008;**5**:1137-58.
6. Friedenstein A, Chailakhyan R, Gerasimov U. Bone

marrow osteogenic stem cells: in vitro cultivation and transplantation in diffusion chambers. *Cell proliferation* 1987;**20**:263-72.

7. Matassi F, Nistri L, Paez DC, Innocenti M. New biomaterials for bone regeneration. *Clinical cases in mineral and bone metabolism* 2011;**8**:21.
8. Zhu N, Chen X. Biofabrication of tissue scaffolds. *Advances in biomaterials science and biomedical applications: InTech*;2013.
9. Cameron R, Kamvari-Moghaddam A. Synthetic bioresorbable polymers. Durability and reliability of medical polymers: *Elsevier*;2012;96-118.
10. Rudnik E. Compostable Polymer Properties and Packaging Applications. Plastic Films in Food Packaging: *Elsevier*;2013;217-48.
11. Haj J, Haj Khalil T, Falah M, *et al*. An ECM-Mimicking, Mesenchymal Stem Cell-Embedded Hybrid Scaffold for Bone Regeneration. *BioMed research international* 2017;**2017**.
12. Rude RK, Gruber HE. Magnesium deficiency and osteoporosis: animal and human observations. *The Journal of nutritional biochemistry* 2004;**15**:710-6.
13. Webster TJ, Ergun C, Doremus RH, Bizios R. Hydroxylapatite with substituted magnesium, zinc, cadmium, and yttrium. II. Mechanisms of osteoblast adhesion. Journal of Biomedical Materials Research: An Official Journal of The Society for Biomaterials, The Japanese Society for Biomaterials, and *The Australian Society for Biomaterials and the Korean Society for Biomaterials* 2002;**59**:312-7.
14. Loh KP, Bao Q, Eda G, Chhowalla M. Graphene oxide as a chemically tunable platform for optical applications. *Nature chemistry* 2010;**2**:1015.
15. Chen H, Müller MB, Gilmore KJ, *et al*. Mechanically strong, electrically conductive, and biocompatible graphene paper. *Advanced Materials* 2008;**20**:3557-61.
16. Nayak TR, Andersen H, Makam VS, *et al*. Graphene for controlled and accelerated osteogenic differentiation of human mesenchymal stem cells. *ACS nano* 2011;**5**:4670-8.
17. Tatavarty R, Ding H, Lu G, *et al*. Synergistic acceleration in the osteogenesis of human mesenchymal stem cells by graphene oxide–calcium phosphate nanocomposites. *Chemical Communications* 2014;**50**:8484-7.
18. Park J, Park S, Ryu S, *et al*. Graphene–regulated cardiomyogenic differentiation process of mesenchymal stem cells by enhancing the expression of extracellular matrix proteins and cell signaling molecules. *Advanced healthcare materials* 2014;**3**:176-81.
19. Biggs M, Richards R, McFarlane S, *et al*. Adhesion formation of primary human osteoblasts and the functional response of mesenchymal stem cells to 330 nm deep microgrooves. *Journal of the Royal Society Interface* 2008;**5**:1231-42.
20. Biggs MJ, Richards R, Gadegaard N, *et al*. Regulation of implant surface cell adhesion: Characterization and quantification of S-phase primary osteoblast adhesions on biomimetic nanoscale substrates. *Journal of Orthopaedic Research* 2007;**25**:273-82.
21. Suryavanshi A, Khanna K, Sindhu K, *et al*. Magnesium oxide nanoparticle-loaded polycaprolactone composite electrospun fiber scaffolds for bone–soft tissue engineering applications: in-vitro and in-vivo evaluation. *Biomedical Materials* 2017;**12**:055011.
22. Dalby MJ, Gadegaard N, Herzyk P, *et al*. Nanomechanotransduction and interphase nuclear organization influence on genomic control. *Journal of cellular biochemistry* 2007;**102**:1234-44.
23. Song J, Gao H, Zhu G, *et al*. The preparation and characterization of polycaprolactone/graphene oxide biocomposite nanofiber scaffolds and their application for directing cell behaviors. *Carbon* 2015;**95**:1039-50.
24. Lee WC, Lim CHY, Shi H, *et al*. Origin of enhanced stem cell growth and differentiation on graphene and graphene oxide. *ACS nano* 2011;**5**:7334-41.
25. Chatakun P, Núñez-Toldrà R, López ED, *et al*. The effect of five proteins on stem cells used for osteoblast differentiation and proliferation: a current review of the literature. *Cellular and molecular life sciences* 2014;**71**:113-42.
26. Huang W, Yang S, Shao J, Li Y-P. Signaling and transcriptional regulation in osteoblast commitment and differentiation. *Frontiers in bioscience: a journal and virtual library* 2007;**12**:3068.
27. Granéli C, Thorfve A, Ruetschi U, *et al*. Novel markers of osteogenic and adipogenic differentiation of human bone marrow stromal cells identified using a quantitative proteomics approach. *Stem cell research* 2014;**12**:153-65.
28. Ogawa E, Maruyama M, Kagoshima H, *et al*. PEBP2/PEA2 represents a family of transcription factors homologous to the products of the Drosophila runt gene and the human AML1 gene. *Proceedings of the National Academy of Sciences* 1993;**90**:6859-63.
29. Franceschi RT, Xiao G. Regulation of the osteoblast-specific transcription factor, Runx2: Responsiveness to multiple signal transduction pathways. *Journal of cellular biochemistry* 2003;**88**:446-54.
30. James AW. Review of signaling pathways governing MSC osteogenic and adipogenic differentiation. *Scientifica* 2013;**2013**.
31. Frantz C, . Stewart KM, Weaver VM. The extracellular matrix at a glance. *J Cell Sci* 2010;**123**: 4195-4200.
32. Sodek J. Chen J, Nagata T, *et al*., Regulation of osteopontin expression in osteoblasts. *Annals of the New York Academy of Sciences* 1995;**760**:223-41.